



## S-shaped heat capacity in an odd–odd deformed nucleus

Balaram Dey<sup>a,\*</sup>, N. Quang Hung<sup>b</sup>, Deepak Pandit<sup>c</sup>, Srijit Bhattacharya<sup>d</sup>, N. Dinh Dang<sup>e</sup>,  
L.T. Quynh Huong<sup>f,g</sup>, Debasish Mondal<sup>c</sup>, S. Mukhopadhyay<sup>c</sup>, Surajit Pal<sup>c</sup>, A. De<sup>h</sup>,  
S.R. Banerjee<sup>i</sup>

<sup>a</sup> Saha Institute of Nuclear Physics, 1/AF-Bidhannagar, Kolkata, 700064, India

<sup>b</sup> Institute of Fundamental and Applied Sciences, Duy Tan University, Ho Chi Minh City 700000, Viet Nam

<sup>c</sup> Variable Energy Cyclotron Centre, 1/AF-Bidhannagar, Kolkata, 700064, India

<sup>d</sup> Department of Physics, Barasat Govt. College, Barasat, N 24 Pgs, Kolkata, 700124, India

<sup>e</sup> Quantum Hadron Physics Laboratory, RIKEN Nishina Center for Accelerator-Based Science, RIKEN, 2-1 Hirosawa, Wako city, Saitama 351-0198, Japan

<sup>f</sup> Department of Natural Science and Technology, University of Khanh Hoa, Nha Trang City, Khanh Hoa Province 652124, Viet Nam

<sup>g</sup> Faculty of Physics and Engineering Physics, Vietnam National University Ho Chi Minh City – University of Science, Ho Chi Minh City 748355, Viet Nam

<sup>h</sup> Department of Physics, Raniganj Girls' College, Raniganj, 713358, India

<sup>i</sup> (Ex)Variable Energy Cyclotron Centre, 1/AF-Bidhannagar, Kolkata, 700064, India



### ARTICLE INFO

#### Article history:

Received 30 October 2018

Received in revised form 30 November 2018

Accepted 4 December 2018

Available online 6 December 2018

Editor: V. Metag

#### Keywords:

Nuclear thermodynamics

Statistical model calculation

Pairing phase transition

### ABSTRACT

We examine the thermodynamic properties of mass  $A \sim 200$  nuclei utilizing angular momentum ( $J$ ) gated nuclear level densities (NLDs) extracted in the excitation energy range of 2–15 MeV. Interestingly, the experimental NLDs are in good agreement with the results of a microscopic approach, which is derived based on the exact pairing plus the independent-particle model at finite temperature (EP + IPM), whereas the conventional Hartree–Fock BCS (HFBCS) and Hartree–Fock–Bogoliubov plus combinatorial method (HFBC) fail to describe these data. Consequently, the thermodynamic properties of those nuclei at finite angular momentum have been extracted using the EP + IPM NLDs. While the heat capacities of  $^{200}\text{Tl}$ ,  $^{211}\text{Po}$  and  $^{212}\text{At}$  (near spherical nuclei) follow the trend as expected in odd–odd and even–odd masses, surprisingly an S-shaped heat capacity is found in odd–odd deformed nucleus  $^{184}\text{Re}$ . It has been shown that this S-shaped heat capacity observed in  $^{184}\text{Re}$  is caused by not only the breaking of nucleon Cooper pairs but also the change of pairing induced by deformation.

© 2018 The Authors. Published by Elsevier B.V. This is an open access article under the CC BY license (<http://creativecommons.org/licenses/by/4.0/>). Funded by SCOAP<sup>3</sup>.

A long-standing problem in nuclear physics is the experimental observation of the pairing phase transition in atomic nuclei. Thermodynamic properties like superfluidity and pairing phase transition are well-established facts in infinite nuclear matter [1], e.g. the core of neutron star. The recent observation of rapid cooling of pulsars, e.g. Cassiopeia A, has been interpreted in terms of superfluidity and neutron triplet pairing [2]. However, these properties digress from infinite nuclear matter to finite nucleus due to the statistical fluctuations in the order parameter. Therefore, the gradual transition from strongly correlated paired states to unpaired ones in atomic nuclei may not be as evident as in infinite matters [1]. This induces a high degree of interests in the study

of nuclear thermodynamics, especially in the energy domain of neutron binding. On the other hand, in finite nuclei it has been seen that the neutron pairing gap depends upon shell and sub-shell closures [3]. Again, new shell closures emerge and older ones disappear in exotic nuclei. Therefore, it will not be an exaggeration to say the role of shell effects on the nuclear pairing is highly important [4]. Although such theoretical studies were done in the past [5], yet experimental investigations are very rare in the existing literature. Similarly, the relationship between nuclear deformation and pairing has not been studied in much detail at higher excitation energies. Calculations within the relativistic mean field (RMF) [6], finite-temperature Hartree–Fock (FTHF) [7], Dirac–Hartree–Fock–Bogoliubov (DHFB) [8,9], etc., have been carried out in the past to understand the effect of deformation on pairing and nuclear thermodynamics. But experimental data are still very scarce in terms of the dependence of angular momentum and deformation on nuclear pairing.

\* Corresponding author.

E-mail addresses: [dey.balaram@gmail.com](mailto:dey.balaram@gmail.com) (B. Dey), [nqhungdtu@gmail.com](mailto:nqhungdtu@gmail.com) (N. Quang Hung).

The study of thermodynamics of finite nuclei involves the reliable extraction of experimental nuclear level density (NLD). Experimental determination of NLDs has been difficult in the past due to the absence of suitable experimental techniques. Recently, the thermal properties of some nuclei ( $^{56,57}\text{Fe}$  [10],  $^{91-98}\text{Mo}$  [11,12],  $^{116,117}\text{Sn}$  [13],  $^{148,149}\text{Sm}$  [14],  $^{161,162}\text{Dy}$  [15,16],  $^{166,167}\text{Er}$  [16,17],  $^{172,173}\text{Yb}$  [18]) were measured by the Oslo group using a new technique, called the Oslo method, and the S-shaped canonical heat capacity has been extracted, signaling the pairing phase transition around the critical temperature of  $T_c = 0.5\text{--}1.0$  MeV. The NLDs and thermodynamical properties of Pt and Au isotopes were also studied in Ref. [19]. In the Oslo technique, the NLD has been extracted from the primary  $\gamma$ -ray spectra measured in coincidence with the particle using inelastic and/or transfer reactions [20]. However, this method is limited only up to low excitation energy  $E^*$  (below the particle threshold) and angular momentum  $J$  (only a few  $\hbar$ ). This limitation in  $E^*$  and  $J$  has recently been overcome by measuring the NLD from the evaporated particle spectra in the compound nuclear reactions [21–23]. Although the major problem connected with this particle evaporation technique is the possible contribution from the multistep and direct reactions, the use of low-energy light-ion beam has provided an excellent scope for extracting the NLD from a particular nuclear decay channel and the contributions from the direct reaction could be ruled out by measuring the particle spectra at backward angles [23]. Fusion reactions with alpha particles populate the compound nucleus in the same isospin states as that of the target nucleus. However, it has been shown earlier by A. Voinov et al., [22] that the extracted level densities from the experimental neutron evaporation spectrum with deuteron beam ( $T_z = 0$ ) gives the same level density as that obtained by using  $^3\text{He}$  beam ( $T_z = 1/2$ ) and the discrete level densities as obtained from RIPL.

On the other hand, the measured NLD (up to the particle threshold) in the Oslo technique was compared with the Constant-Temperature formula [24] and then extrapolated up to the higher energy using the Fermi-gas (FG) model [25] to estimate the thermodynamic quantities. However, the functional form of the NLD is till date not adequately known due to the lack of availability of experimental data at higher  $E^*$  and  $J$ . Therefore the use of a single consistent theoretical calculation, instead of adding two different phenomenological models, to investigate the thermodynamic properties of atomic nuclei based on the measured NLDs below and above the particle threshold could be a better choice. Very recently, the NLD has been measured in a  $^{96}\text{Tc}$  nucleus below and much above the particle threshold energy at different  $J$ -values using the particle evaporation technique and compared with the aid of a consistent theoretical calculation, namely the exact pairing plus independent-particle model at finite temperature (EP + IPM) [23]. Thus, the angular momentum gated thermodynamic parameters could be estimated. In addition, till now most of the thermal properties have been studied in the nuclei where the shell effect ( $\delta S$ ) is very small (less than  $\sim 1$  MeV). The large shell effect ( $\delta S \sim 10$  MeV) mass region has rarely been studied and thus it is very important to investigate how the thermodynamic properties behave because of the large effect of nuclear shells.

In this Letter, the NLDs and, consequently, the nuclear thermodynamic quantities (TQ) for four different nuclei ( $^{184}\text{Re}$ ,  $^{200}\text{Tl}$ ,  $^{211}\text{Po}$ , and  $^{212}\text{At}$ ) are estimated. Those nuclei are chosen so as to understand the shell and deformation effects on the TQ.  $^{184}\text{Re}$  is deformed with small shell effect (quadrupole deformation parameter  $\beta_2 = 0.23$  with  $\delta S = -2.06$ ), whereas other three nuclei have larger shell effects ( $\delta S = -7.32$ ,  $-9.56$  and  $-8.42$  for  $^{200}\text{Tl}$ ,  $^{211}\text{Po}$ , and  $^{212}\text{At}$ , respectively) but with almost zero deformation [26]. In addition, the effect of even-odd ( $^{211}\text{Po}$ ) and odd-odd ( $^{212}\text{At}$ ) pair-

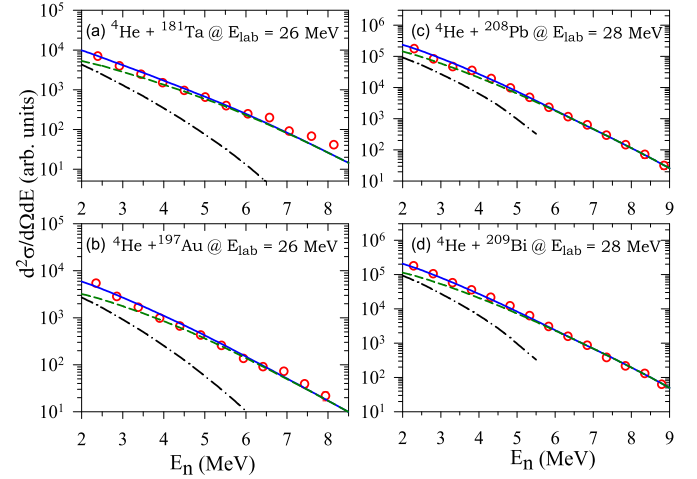


**Fig. 1.** Experimental neutron energy spectra (symbols) along with the CASCADE calculations (solid lines) taken from Refs. [27,28]. The dashed and dashed-dotted lines represent the contributions from 1n and 2n channels, respectively.

ing correlations on the thermodynamic properties of atomic nuclei has also been investigated.

In the present work the NLD have been extracted using the previously reported neutron evaporation spectra at low excitation energies by K. Banerjee et al., [27] and Pratap Roy et al., [28], where the experiments were performed using the  $\alpha$ -beams from the K-130 cyclotron at VECC. The compound nuclei  $^{185}\text{Re}$ ,  $^{201}\text{Tl}$ ,  $^{212}\text{Po}$ , and  $^{213}\text{At}$  were populated at different initial excitation energies ( $E^* \sim 18\text{--}50$  MeV) in the reactions  $^4\text{He} + ^{181}\text{Ta}$ ,  $^4\text{He} + ^{197}\text{Au}$ ,  $^4\text{He} + ^{208}\text{Pb}$  and  $^4\text{He} + ^{209}\text{Bi}$ , respectively to investigate the shell and collective effects in NLD. The lowest excitation energy data of 23.2, 23.9, 18.5 and 18.2 MeV for  $^{185}\text{Re}$ ,  $^{201}\text{Tl}$ ,  $^{212}\text{Po}$ , and  $^{213}\text{At}$ , respectively have been used to extract the NLDs to study the thermodynamic properties.

It should be pointed out that the neutron energy spectra should have a negligible contamination from the non-compound reactions to obtain the NLD using particle spectra. Hence, the neutron spectra at the most backward angle ( $150^\circ$ ) were used to extract the inverse level density parameter earlier [27,28]. The previous studies [27,28] also confirmed that the neutron energy spectra measured at backward angles from alpha induced reactions in different mass regions are mainly dominated by the compound nuclear (CN) reactions. In order to identify the pre-dominant contributor, the neutron evaporation spectra from different nuclei in the decay chain of the CN were extracted from the CASCADE code [29] and are shown in Fig. 1 along with the experimental data. It was found that the contribution of the neutron energy  $E_n > 3$  MeV is mainly dominated by 1n channel and enables us to extract the experimental NLD using the approach presented in Ref. [23].

The experimental NLD was extracted using the relation following the approach presented in Refs. [21,30,31], namely

$$\rho_{\text{exp}}(E_X) = \rho_{\text{fit}}(E_X) \frac{(d\sigma/dE)_{\text{exp}}}{(d\sigma/dE)_{\text{fit}}} \quad (1)$$

Here,  $(d\sigma/dE)_{\text{exp}}$  and  $(d\sigma/dE)_{\text{fit}}$  are the experimental neutron evaporation and best-fit theoretical spectra taken from Refs. [27, 28], respectively. The quantity  $\rho_{\text{fit}}(E_X)$  is the best-fit level density taken from the CASCADE calculation [29], which is given by

$$\rho(E_X, J) = \frac{2J + 1}{12\theta^{3/2}} \sqrt{a} \frac{\exp(2\sqrt{a}U)}{U^2} \quad (2)$$

Here,  $\theta = \frac{2I_{\text{eff}}}{\hbar^2}$ ,  $I_{\text{eff}}$  is the effective rigid-body moment of inertia,  $E_X = U - E_n^{\text{CM}} - S_n$  is the effective excitation energy, where  $E_n^{\text{CM}}$

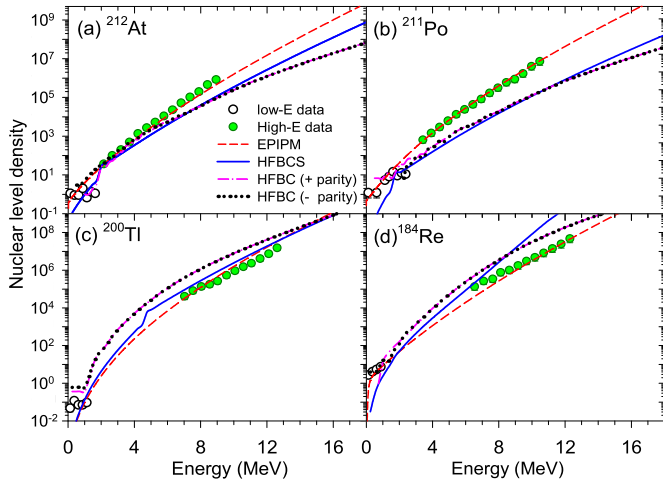


**Fig. 2.** Angular momentum gated NLDs along with the results of different theoretical calculations for  $J = 12 \hbar$ . Filled symbols are the extracted NLDs in the present work and open symbols are taken from Ref. [37] weighted over our  $J$ -distribution.

is the neutron energy in the center-of-mass frame,  $S_n$  is the neutron separation energy;  $U = E^* - \frac{J(J+1)}{\theta} - \Delta P$ , where  $\Delta P$  is the pairing energy term, and  $E^*$  is the initial excitation energy. The level density parameter “ $a$ ” was deduced from the experimentally determined asymptotic NLD parameter  $\tilde{a}$  by using the Ignatyuk’s parameterization [32] given by

$$a = \tilde{a} \left[ 1 + \frac{\delta S}{U} [1 - \exp(-\gamma U)] \right], \quad (3)$$

where,  $\gamma = \frac{0.4A^{4/3}}{\tilde{a}}$  is the rate at which the shell effect is damped with increasing the excitation energy. The values of the ground-state shell correction  $\delta S$  are defined as the differences of the experimental and theoretical (liquid drop) masses, and mentioned previously for the four selected nuclei. The extracted values for inverse level density parameter ( $k = A/\tilde{a}$ ) are  $9.7 \pm 0.7$ ,  $10.0 \pm 0.7$ ,  $7.8 \pm 0.4$  and  $8.3 \pm 0.3$  MeV for  $^{184}\text{Re}$ ,  $^{200}\text{Tl}$ ,  $^{211}\text{Po}$  and  $^{212}\text{At}$ , respectively [27,28]. In this way, the NLDs at different excitation energies for finite angular momentum are extracted (as shown in Fig. 2) and further used to investigate the thermal properties of atomic nuclei.

An atomic nucleus can be assumed as a statistical ensemble because of a very high density of states even at low excitation energy (few MeV). The NLD is directly related to the partition function of the statistical ensemble, which is a fundamental quantity describing the statistical properties of a system in thermodynamic equilibrium. Most of other TQs can be expressed in terms of this partition function or its derivative. In principle, the thermodynamic properties of nuclear system can be described based on the grand canonical ensemble (GCE), canonical ensemble (CE), or microcanonical ensemble (MCE) [33]. In this work, the CE has been used in order to investigate the thermodynamical properties of all selected nuclei. The expression of the CE partition function is given by

$$Z(T, J) = \sum_{E_n=0}^{E_n} \rho(E_n, J) e^{-\frac{E_n}{T}} \delta E_n, \quad (4)$$

where  $\rho(E_n, J)$  is the NLD at  $E_n = E_n$  and total angular momentum  $J$ , and  $\delta E_n$  is the energy interval. The free energy  $F$ , average energy  $\bar{E}$ , entropy  $S$ , and heat capacity  $C$  can be expressed based on the CE partition function (4) as  $F = -T \ln Z$ ,  $S = -\partial F / \partial T$ ,  $\bar{E} = F + TS$ , and  $C = \partial \bar{E} / \partial T$ . Formally, the calculation using eqn.

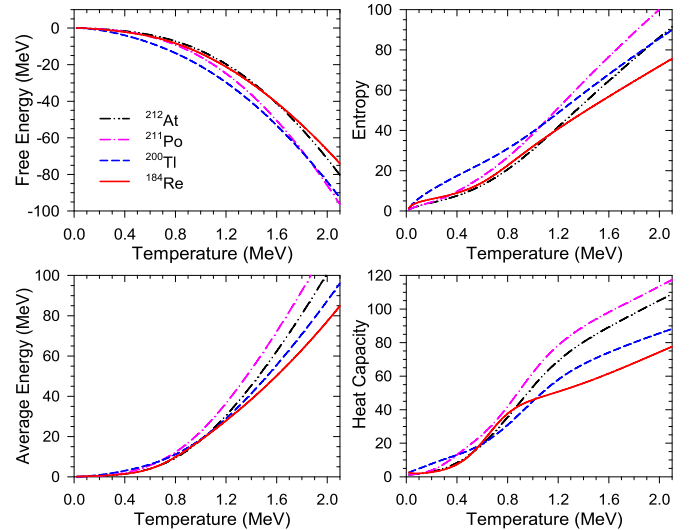


**Fig. 3.** Angular-momentum-gated thermodynamic quantities as functions of temperature obtained by using the EP + IPM level densities for  $J = 12 \hbar$ .

(4) requires an infinite summation. However, the extracted NLDs in Fig. 2 only cover the excitation energy up to 15 MeV. Therefore, the extracted NLD has been compared with the different theoretical calculations such as the EP + IPM [34], HFBCS [35], and HFBC for positive and negative parities [36]. Finally, the best matched theoretical NLD has been used to investigate the thermal properties of atomic nuclei. Details of the theoretical calculation employed in the present work are discussed in Ref. [23].

The experimental angular momentum gated NLDs compared with the results of different microscopic calculations (EP + IPM, HFBCS, and HFBC) are shown in Fig. 2. The level density parameter and angular momentum are measured in the experiment and used in the statistical model calculation to extract the NLD. The uncertainty in the NLD due to the statistical model parameters has been checked and found to be  $\sim 5$ –10%. The error due to  $J$ -distribution ( $\pm 4 \hbar$ ) has been taken care of by using the extracted NLD weighted over the experimental  $J$ -distribution. The low-energy NLD data ( $\sim 1$  MeV, represented by the open circles in Fig. 2) are obtained from the total NLD taken from Ref. [37]. The latter is determined by counting the numbers of experimental discrete levels in the low-energy region. These low-energy data are then multiplied by the spin distribution  $f(J) = (2J+1) \exp[-J(J+1)/2\sigma^2] / (2\sigma^3 \sqrt{2\pi})$  with  $\sigma^2$  being the spin cut-off factor taken from the systematics [38] and weighted over the experimental angular-momentum distribution for a proper comparison with the high-energy data. An overall agreement between the experimental data and the predictions by the EP + IPM calculations is clearly observed, while the HFBCS and HFBC can not explain the data. It should be mentioned here that no normalization is required within the EP + IPM calculations when comparing with the extracted NLD. As the EP + IPM results match well with the data, this model is further used to calculate the thermodynamic quantities of four selected nuclei at  $J = 12 \hbar$ .

Fig. 3 shows the Helmholtz free energy  $F$ , average excitation energy  $\bar{E}$ , entropy  $S$ , and heat capacity  $C$  as a function of  $T$ .  $F$  and  $\bar{E}$  behave smoothly with varying  $T$  for all the nuclei. However,  $S$  and  $C$  show different variations with  $T$ . The entropies of  $^{211}\text{Po}$  (odd–even),  $^{212}\text{At}$  (odd–odd), and  $^{184}\text{Re}$  (odd–odd) have similar values below 1 MeV but diverge thereafter. On the other hand, the entropy of  $^{200}\text{Tl}$  (odd–odd) is almost a factor of 2 higher compared to the other nuclei below  $T = 0.5$  MeV, but increases slowly beyond  $T = 0.9$  MeV. This change in entropy appears primarily due to the different shell structures of the nuclei at low  $T$  since

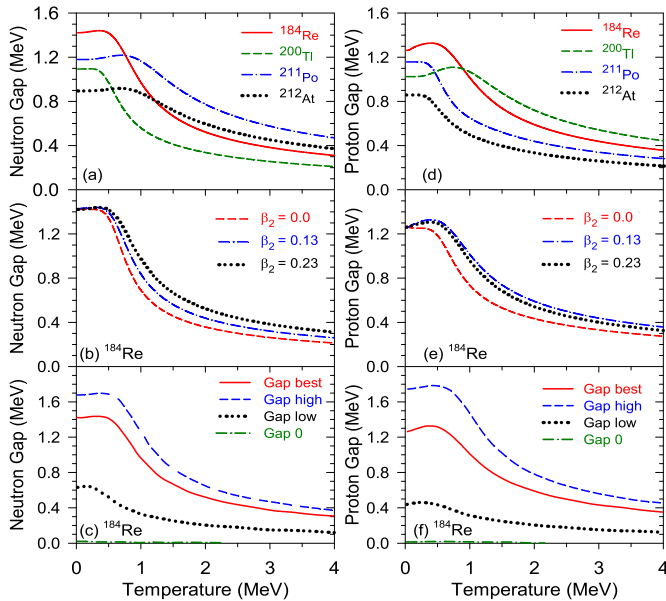


**Fig. 4.** Exact pairing gaps (without angular momentum or  $J = 0$ ) as functions of temperature for  $^{184}\text{Re}$  under consideration [a, d], at different deformations for  $^{184}\text{Re}$  [b, e], and using different values of pairing gaps at zero temperature for  $^{184}\text{Re}$  [c, f].

they show smooth variation at higher  $T$  (above  $T = 1.6$  MeV), where the shell structures are predicted to be melted [32,39,40]. Most noteworthy is the nature of heat capacity for  $^{184}\text{Re}$ , which is completely different from the other three nuclei. There is a pronounced bump ( $S$ -shape) in the heat capacity of  $^{184}\text{Re}$  at around  $T \sim 0.8$  MeV, which is close to the critical temperature  $T_c$ , where the pairing gap collapses as predicted by the conventional BCS theory. This  $S$ -shape in the heat capacity is interpreted as a fingerprint for pairing transition in nuclei. The heat capacities  $^{211}\text{Po}$ ,  $^{212}\text{At}$ , and  $^{200}\text{Tl}$  do not show the pronounced  $S$ -shape structure as expected for odd–odd and odd–even nuclei. It is also interesting to note that the heat capacities of the isotones  $^{211}\text{Po}$  and  $^{212}\text{At}$  show very similar behavior and adding one proton only slightly reduces the heat capacity in this mass region.

In order to understand the difference in the heat capacities, the exact neutron and proton pairing gaps have been calculated as functions of  $T$  as shown in Figs. 4(a) and (d). Although these exact gaps are obtained only for the non-rotating case (without angular momentum or  $J = 0$ ), they are predicted to decrease with increasing  $J$ . However, the difference between the gaps for  $J = 0$  and  $12 \hbar$ , as shown in Fig. 4, should be very small [41–43]. It is seen that the exact pairing gaps change differently with  $T$ . The gap at  $T < 1$  MeV for  $^{184}\text{Re}$  is quite larger than that of other nuclei and it also has the steepest slope. As  $^{184}\text{Re}$  nucleus is deformed ( $\beta_2 = 0.23$ ), its pairing gaps have been calculated at different deformations as shown in Figs. 4(b) and (e). As can be seen from these figures, the pairing gaps with  $\beta_2 = 0$  (no deformation) have the steepest slope. Consequently, the heat capacity for  $\beta_2 = 0$  (and  $J = 12 \hbar$ ) shows a clear  $S$ -shape as seen in Fig. 5(a). However, the NLD for  $\beta_2 = 0$  does not match the experimental data as shown in Fig. 5(c). Next, the heat capacity for  $^{184}\text{Re}$  has been calculated by keeping  $\beta_2 = 0.23$  and changing the pairing gaps such as high gap, best gap, low gap, and nearly zero gap as shown in Figs. 4(c) and (f). The heat capacities at low and zero gaps do not show the  $S$ -shape and the corresponding NLDs do not fit the data, while those at high gap and best gap show a clear  $S$ -shape as seen in Fig. 5(b). It should be mentioned here that the NLD for best gap matches experimental data well and was considered for the

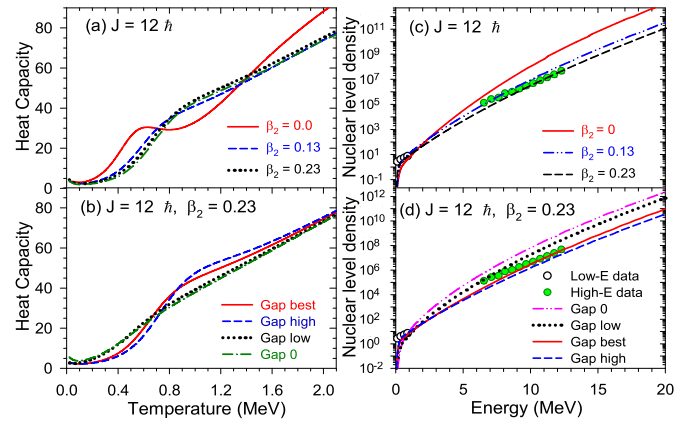


**Fig. 5.** [a, b] Heat capacities as functions of temperature at different deformations and pairing gaps for  $^{184}\text{Re}$  nucleus. [c, d] Extracted NLDs along with the EP + IPM calculations at different deformations and pairing gaps for  $^{184}\text{Re}$  nucleus. The dashed-dotted lines in [a] stand for the results obtained within the EP + IPM without the collective enhancement factor.

thermodynamic calculation. To see if the collective enhancement contributes in causing the  $S$ -shape heat capacity for  $^{184}\text{Re}$  [27,44], the NLD calculations within the EP + IPM were carried out by setting the collective enhancement factors  $k_{\text{rot}}$  and  $k_{\text{vib}}$  [34] equal to 1. The obtained results (dash-dotted lines in Fig. 5(a)) show that the  $S$ -shape of the heat capacity remains, that is the collective enhancement plays no role in this issue. Therefore, it can be concluded that the  $S$ -shape of heat capacity seen in  $^{184}\text{Re}$  at  $J = 12 \hbar$  is only due to the change of pairing gaps caused by the change of deformation.

In summary, nuclear level densities of odd–odd and odd–even nuclei in  $A \sim 200$  have been extracted by utilizing the neutron evaporation energy spectra of Refs. [27,28] measured using the low-energy  $\alpha$  beam. The microscopic EP + IPM calculation explains well all the experimental data in this mass region and, consequently, is used to study the thermodynamic properties of  $^{184}\text{Re}$ ,  $^{200}\text{Tl}$ ,  $^{211}\text{Po}$ , and  $^{212}\text{At}$  nuclei. While the heat capacities of  $^{200}\text{Tl}$ ,  $^{211}\text{Po}$ , and  $^{212}\text{At}$ , which are nearly spherical, display the correct behavior as expected in case of even–odd/odd–odd systems, a pronounced  $S$ -shaped heat capacity is observed for an odd–odd deformed  $^{184}\text{Re}$  nucleus. It has been shown that this observed  $S$ -shape in the heat capacity of  $^{184}\text{Re}$  is due to the change of pairing gaps caused by the change of deformation. Thus, it would be very interesting to extract the NLDs and study the thermodynamic properties of different deformed nuclei in a systematic way in near future.

## Acknowledgements

The authors are very grateful to Dr. Pratap Roy for providing the experimental neutron energy spectra. The numerical calculations within the EP + IPM, which were carried out using the FORTRAN IMSL Library by Visual Numerics on the RIKEN supercomputer HOKUSAI-GreatWave System, are supported by the National Foundation for Science and Technology Development (NAFOSTED) of Vietnam through Grant No. 103-04.2017.323. Balaram Dey acknowledges financial support from the SERB-NPDF (India), SERB/PDF/2017/000246.

## References

- [1] A. Belic, D.J. Dean, M. Hjorth-Jensen, Nucl. Phys. A 731 (2004) 381.
- [2] D. Page, M. Prakash, J.M. Lattimer, A.W. Steiner, Phys. Rev. Lett. 106 (2011) 081101.

- [3] Y.F. Niu, Z.M. Niu, N. Paar, D. Vretenar, G.H. Wang, J.S. Bai, J. Meng, *Phys. Rev. C* 88 (2013) 034308.
- [4] R.V.F. Janssens, *Nature* 459 (2009) 1069.
- [5] R. Lisboa, M. Malheiro, B.V. Carlson, *Phys. Rev. C* 93 (2016) 024321.
- [6] B.K. Agrawal, Tapas Sil, S.K. Samaddar, J.N. De, *Phys. Rev. C* 63 (2001) 024002.
- [7] J.L. Egido, L.M. Robledo, V. Martin, *Phys. Rev. Lett.* 85 (2000) 26.
- [8] P. Bonche, S. Levit, D. Vautherin, *Nucl. Phys. A* 427 (1984) 278.
- [9] B.V. Carlson, D. Hirata, *Phys. Rev. C* 62 (2000) 054310.
- [10] E. Algin, et al., *Phys. Rev. C* 78 (2008) 054321.
- [11] R. Chankova, et al., *Phys. Rev. C* 73 (2006) 034311.
- [12] K. Kaneko, et al., *Phys. Rev. C* 74 (2006) 024325.
- [13] U. Agvaanluvsan, et al., *Phys. Rev. C* 79 (2009) 014320.
- [14] S. Siem, et al., *Phys. Rev. C* 65 (2002) 044318.
- [15] M. Guttormsen, et al., *Phys. Rev. C* 62 (2000) 024306.
- [16] E. Melby, et al., *Phys. Rev. Lett.* 83 (1999) 3150.
- [17] E. Melby, et al., *Phys. Rev. C* 63 (2001) 044309.
- [18] A. Schiller, et al., *Phys. Rev. C* 63 (2001) 021306(R).
- [19] F. Giacoppo, et al., *Phys. Rev. C* 90 (2014) 054330.
- [20] A. Schiller, et al., *Nucl. Instrum. Methods Phys. Res., Sect. A* 447 (2000) 498.
- [21] A.V. Voinov, et al., *Phys. Rev. C* 77 (2008) 034613.
- [22] A.V. Voinov, et al., *Phys. Rev. C* 74 (2006) 014314.
- [23] Balaram Dey, et al., *Phys. Rev. C* 96 (2017) 054326.
- [24] T. Ericson, *Nucl. Phys. A* 11 (1959) 481.
- [25] H.A. Bethe, *Phys. Rev.* 50 (1936) 332;  
H.A. Bethe, *Rev. Mod. Phys.* 9 (1937) 69.
- [26] P. Moller, et al., *At. Data Nucl. Data Tables* 109–110 (2016) 1–204.
- [27] K. Banerjee, et al., *Phys. Lett. B* 772 (2017) 105.
- [28] P. Roy, et al., *Phys. Rev. C* 94 (2016) 064607.
- [29] F. Pühlhofer, et al., *Nucl. Phys. A* 280 (1976) 267.
- [30] D.R. Chakrabarty, et al., *Phys. Rev. C* 51 (1995) 2942.
- [31] A.P.D. Ramirez, et al., *Phys. Rev. C* 88 (2013) 064324.
- [32] A.V. Ignatyuk, G.N. Smirenkin, A.S. Tishin, *Sov. J. Nucl. Phys.* 21 (1975) 255.
- [33] N. Quang Hung, N. Dinh Dang, *Phys. Rev. C* 81 (2010) 057302;  
N. Quang Hung, N. Dinh Dang, *Phys. Rev. C* 82 (2010) 044316.
- [34] N. Quang Hung, N. Dinh Dang, L.T. Quynh Huong, *Phys. Rev. Lett.* 118 (2017) 022502.
- [35] P. Demetriou, S. Goriely, *Nucl. Phys. A* 695 (2001) 95.
- [36] S. Hilaire, S. Goriely, *Nucl. Phys. A* 779 (2006) 63;  
S. Goriely, S. Hilaire, A.J. Koning, *Phys. Rev. C* 78 (2008) 064307.
- [37] <https://www-nds.iaea.org/RIPL-3/>.
- [38] R. Capote, et al., *Nucl. Data Sheets* 110 (2009) 3107.
- [39] A. Bohr, B. Mottelson, *Nuclear Structure*, vol. II, Benjamin, New York, 1975.
- [40] F.A. Ivanyuk, C. Ishizuka, M.D. Usang, S. Chiba, *Phys. Rev. C* 97 (2018) 054331.
- [41] S. Frauendorf, N.K. Kuzmenko, V.M. Mikhajlov, J.A. Sheikh, *Phys. Rev. B* 68 (2003) 024518.
- [42] D.J. Dean, K. Langanke, H.A. Nam, W. Nazarewicz, *Phys. Rev. Lett.* 105 (2010) 212504.
- [43] N. Quang Hung, N. Dinh Dang, *Phys. Rev. C* 84 (2011) 054324.
- [44] Deepak Pandit, et al., *Phys. Rev. C* 97 (2018) 041301(R).